

TWO CONJECTURES ON THE STOKES COMPLEX IN THREE DIMENSIONS ON FREUDENTHAL MESHES

PATRICK E. FARRELL*, LAWRENCE MITCHELL†, AND L. RIDGWAY SCOTT‡

AMS subject classifications. 35Q30, 76D05, 65N30, 74S05, 76M10

Abstract. In recent years a great deal of attention has been paid to discretizations of the incompressible Stokes equations that exactly preserve the incompressibility constraint. These are of substantial interest because these discretizations are pressure-robust, i.e. the error estimates for the velocity do not depend on the error in the pressure. Similar considerations arise in nearly incompressible linear elastic solids. Conforming discretizations with this property are now well understood in two dimensions, but remain poorly understood in three dimensions. In this work we state two conjectures on this subject. The first is that the Scott–Vogelius element pair is inf-sup stable on uniform meshes for velocity degree $k \geq 4$; the best result available in the literature is for $k \geq 6$. The second is that there exists a stable space decomposition of the kernel of the divergence for $k \geq 5$. We present numerical evidence supporting our conjectures.

1. Introduction. We consider two closely related problems for a bounded Lipschitz domain $\Omega \subset \mathbb{R}^d$, $d \in \{2, 3\}$. The first is the incompressible Stokes equations: given $f \in L^2(\Omega; \mathbb{R}^d)$, find the velocity $u : \Omega \rightarrow \mathbb{R}^d$ and pressure $p : \Omega \rightarrow \mathbb{R}$ such that

$$(1.1a) \quad -\nabla \cdot \varepsilon u + \nabla p = f \quad \text{in } \Omega,$$

$$(1.1b) \quad \nabla \cdot u = 0 \quad \text{in } \Omega,$$

$$(1.1c) \quad u = 0 \quad \text{on } \partial\Omega,$$

where $\varepsilon u = 1/2 (\nabla u + (\nabla u)^T)$ is the symmetric gradient of u . The second is the Navier–Cauchy equation of linear elasticity: given $f \in L^2(\Omega; \mathbb{R}^d)$ and $\gamma > 0$, find the displacement $u : \Omega \rightarrow \mathbb{R}^d$ that satisfies

$$(1.2a) \quad -\nabla \cdot \varepsilon u - \gamma \nabla \nabla \cdot u = f \quad \text{in } \Omega,$$

$$(1.2b) \quad u = 0 \quad \text{on } \partial\Omega.$$

Here $\gamma = 2\lambda/\mu$, where λ and μ are the Lamé parameters. As $\gamma \rightarrow \infty$, the material is said to be nearly incompressible. The term $-\nabla \nabla \cdot u$ in (1.2a) is connected to the incompressibility constraint (1.1b); it arises in the Stokes momentum equation (1.1a) when employing an augmented Lagrangian approach [6] to enforcing the divergence-zero constraint (1.1b).

When discretizing (1.1), it is highly desirable to choose spaces V_h for the velocity and Π_h for the pressure such that all discretely divergence free functions are pointwise divergence free, i.e. the incompressibility constraint (1.1b) is satisfied exactly on the discrete level [27]. Achieving this is difficult; no element pair for exact enforcement is known that is simultaneously inf-sup stable, low-order, conforming, has polynomial basis functions, and is effective on general meshes. On simplicial grids with special mesh structure, it is possible to use the conforming Scott–Vogelius finite element pair $[CG_k]^d$ - DG_{k-1} [48, 49] for $k \geq d$ (for Alfeld splits [39, 22, 17, 52]) or $k \geq d-1$ (for Powell–Sabin splits [20, 53, 55, 21]). The approach of Guzmán and Neilan [22] is conforming, works for arbitrary degree and on general meshes, but requires the use of piecewise polynomial

*Mathematical Institute, University of Oxford, Oxford, England. (patrick.farrell@maths.ox.ac.uk)

†NVIDIA Corporation, Santa Clara, CA, USA. (lmitchell@nvidia.com)

‡Department of Computer Science, University of Chicago, Chicago, USA. (ridg@uchicago.edu). PEF was funded by EPSRC grants EP/R029423/1 and EP/W026163/1.

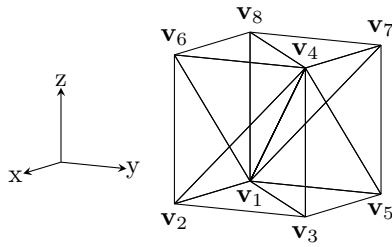


FIG. 2.1. Unit cube for a structured mesh in three dimensions used for computational experiments. Given $N \in \mathbb{N}$, a $N \times N \times N$ mesh of cubes is generated, each of which is subdivided into 6 tetrahedra as shown. Vertex labels correspond to the vertices enumerated in [Appendix A](#).

basis functions on each cell (instead of standard polynomials). Non-conforming divergence-free discretizations are reviewed in John et al. [27, §4.4]. Finally, another approach is to consider the use of high-order discretizations, which are attractive for their advantageous computational properties on modern architectures [49, 48, 37, 54]. Another alternative is to modify the right-hand side of the problem with an operator that maps discretely divergence-free test functions to exactly divergence-free ones [30].

In this paper we state two conjectures regarding the discretization and multigrid solution of (1.1) and (1.2) on structured uniform tetrahedral meshes (Freudenthal meshes [7]). We focus on Freudenthal meshes since some theoretical results are known in this case. For concreteness we briefly describe the Freudenthal triangulation of the unit cube in [Appendix A](#). The first is that the Scott–Vogelius element pair is inf-sup stable on Freudenthal meshes for $k \geq 4$; the best available result is that of Zhang, who proved that the pair is stable for $k \geq 6$ [54]. We conjecture this on the basis of numerical calculations of the inf-sup constant for varying k . These rely on a new algorithm that can compute the inf-sup constant for elements that are divergence-free when an exact characterization of the pressure space is not known. The second is that on the same meshes the subspace $Z_h \subset V_h$ of divergence-free functions admits a local basis defined on the vertex-centred patches for $k \geq 5$, and that the associated space decomposition is stable. This is significant because identifying a local basis for the kernel of the divergence operator is crucial for multigrid algorithms applied to (1.2). We conjecture this on the basis of observed γ -robustness of a multigrid solution algorithm for (1.2), for which the local kernel decomposition is essential [43]. The existence of a local basis is known in three dimensions for Alfeld splits [17] and Worsey–Farin splits [21], but remains an open question for general meshes, and in particular for the Freudenthal meshes considered here.

2. Inf-sup stability of the Scott–Vogelius element. The mixed formulation of (1.1) is to find $(u, p) \in V \times \Pi := H_0^1(\Omega; \mathbb{R}^d) \times L_0^2(\Omega)$ such that

$$(2.1) \quad (\varepsilon u, \varepsilon v)_{L^2} - (p, \nabla \cdot v)_{L^2} - (q, \nabla \cdot u)_{L^2} = (f, v)_{L^2(\Omega)} \quad \text{for all } (v, q) \in V \times \Pi.$$

Define $(T, U)_{L^2(\Omega)} = (T, U)_{L^2}$ for any scalar-, vector-, or tensor-valued functions T, U .

The inf-sup condition determines whether or not a pair of spaces $V_h \subset V$, $\Pi_h \subset \Pi$ in a mixed finite element method provide a compatible discretization [9], since the symmetric gradient term is coercive on V . In the context of (2.1), this condition encapsulates a constraint between the divergence of the velocity space V_h and the

pressure space Π_h : there exists $\beta > 0$ such that

$$(2.2) \quad \beta \sqrt{(q, q)_{L^2(\Omega)}} \leq \sup_{\substack{v \in V_h \\ v \neq 0}} \frac{(\nabla \cdot v, q)_{L^2(\Omega)}}{\sqrt{(\nabla v, \nabla v)_{L^2(\Omega)}}} \quad \forall q \in \Pi_h.$$

In this section we make the following conjecture:

CONJECTURE 1. *Let V_h be constructed with continuous Lagrange elements of degree k , and choose $\Pi_h = \nabla \cdot V_h$. For $k \geq 4$, the inf-sup condition (2.2) holds on structured tetrahedral meshes of the form in Figure 2.1, known as the Freudenthal triangulation [7], with a constant that depends only on k .*

We conjecture this on the basis of numerical computations with a new algorithm for calculating the inf-sup constant, which we now describe.

2.1. Computing the inf-sup constant. There are several methods to estimate computationally the inf-sup constant β for various spaces and variational problems [39, 41, 4]. In [18], approximation of the corresponding Ladyzhenskaya inf-sup constant for the continuous problem is studied. All of these are based on solving eigenproblems.

In [41], an automated system ASCoT was introduced for computing inf-sup constants. It takes as input V_h and Π_h . However, when $\Pi_h = \nabla \cdot V_h$, it is advantageous to exploit this structure in the calculation of the inf-sup constant. More importantly, the space $\nabla \cdot V_h$ may not be known *a priori*, and so a different algorithm is needed that does not require Π_h as input.

A technique was developed by one of the authors in [46] that deals specifically with the $\Pi_h = \nabla \cdot V_h$ case and casts this as an eigenvalue problem, as follows. Define the bilinear forms

$$(2.3) \quad a(u, v) = \int_{\Omega} \nabla u : \nabla v \, dx, \quad b(v, q) = \int_{\Omega} (\nabla \cdot v) q \, dx.$$

First define

$$(2.4) \quad Z_h = \{v \in V_h : b(v, q) = 0 \, \forall q \in \Pi_h\},$$

which is the set of divergence-free functions in V_h since $\Pi_h = \nabla \cdot V_h$. Define κ by

$$(2.5) \quad \kappa = \min_{0 \neq v \in V_h, v \perp_a Z_h} \frac{(\nabla \cdot v, \nabla \cdot v)_{L^2}}{a(v, v)} = \min_{0 \neq v \in Z_h^\perp} \frac{(\nabla \cdot v, \nabla \cdot v)_{L^2}}{a(v, v)},$$

where $v \perp_a Z_h$ means that $a(v, w) = 0$ for all $w \in Z_h$ and

$$(2.6) \quad Z_h^\perp = \{v \in V_h : a(v, w) = 0 \, \forall w \in Z_h\}.$$

We recall the following lemma from [46, Lemma 26.1].

LEMMA 2.1. *Suppose that $\|v\|_V = \sqrt{a(v, v)}$ and $\Pi_h = \nabla \cdot V_h$. Then*

$$(2.7) \quad \beta = \inf_{\substack{q \in \Pi_h \\ q \neq 0}} \sup_{\substack{v \in V_h \\ v \neq 0}} \frac{b(v, q)}{\|v\|_V \|q\|_{L^2}} = \inf_{\substack{q \in \Pi_h \\ q \neq 0}} \sup_{\substack{v \in Z_h^\perp \\ v \neq 0}} \frac{b(v, q)}{\|v\|_V \|q\|_{L^2}} \geq \sqrt{\kappa} \geq \frac{1}{2}\beta,$$

where κ is defined in (2.5).

This result holds also for the bilinear form

$$(2.8) \quad a(u, v) = (\varepsilon u, \varepsilon v)_{L^2(\Omega)},$$

with possibly different constants.

Computing κ is equivalent to finding the smallest eigenvalue λ of the following eigenproblem: find $0 \neq u_h \in Z_h^\perp$ such that

$$(2.9) \quad (\nabla \cdot u_h, \nabla \cdot v_h)_{L^2(\Omega)} = \lambda a(u_h, v_h) \quad \forall v_h \in Z_h^\perp,$$

which is equivalent to the Rayleigh quotient minimization (2.5). Note that $\kappa > 0$ since $\kappa = 0$ leads to the contradiction $\nabla \cdot u_h = 0$, that is, $u_h \in Z_h \cap Z_h^\perp$. Thus there are no spurious modes when $\Pi_h = \nabla \cdot V_h$.

We can write (2.9) in operator form as

$$(2.10) \quad Bu_h = \lambda Au_h.$$

The equation (2.10) is a symmetric generalized eigenvalue problem [50], and its eigenvalues are all real. There are many algorithms for solving symmetric generalized eigenvalue problems [19, 42, 50]. However, we do not have an explicit basis for the space Z_h^\perp , so we choose to use matrix-free methods. Here we focus on a simple method related to the power method.

Since A is invertible on all of V_h , it would be attractive to utilize an iteration in which we invert A , and not B . We introduce a shift σ :

$$(2.11) \quad (B - \sigma A)u_h = \lambda^\sigma Au_h.$$

If $\lambda_1 \leq \lambda_2 \leq \dots \leq \lambda_N$ are the eigenvalues of the symmetric problem (2.10), that is, for the operator $A^{-1}B$, and $\lambda_1^\sigma \leq \lambda_2^\sigma \leq \dots \leq \lambda_N^\sigma$ are the eigenvalues of the shifted problem (2.11), then $\lambda_i^\sigma = \lambda_i - \sigma$ for all $i = 1, \dots, N$. Moreover, λ_i^σ are the eigenvalues for the operator $A^{-1}B - \sigma I$, and the eigenvectors u_h^i for λ_i^σ and λ_i are the same, for all $i = 1, \dots, N$.

2.2. Using the power method. We can solve for certain eigenvalues and eigenvectors u_h via the power method [45] for (2.11), namely to find $u^n \in Z_h^\perp$ such that

$$(2.12) \quad \begin{aligned} a(u^n, v_h) &= (\nabla \cdot \hat{u}^{n-1}, \nabla \cdot v_h)_{L^2(\Omega)} - \sigma a(\hat{u}^{n-1}, v_h) \quad \forall v_h \in Z_h^\perp \\ \lambda^{n+1} &= \frac{(\nabla \cdot u^n, \nabla \cdot u^n)_{L^2(\Omega)}}{a(u^n, u^n)}, \quad \hat{u}^n = (\|u^n\|_V)^{-1} u^n. \end{aligned}$$

The choices of initial iterate and termination criterion are discussed subsequently.

We now consider how to compute this, despite the fact that the space Z_h^\perp is not explicitly known. Suppose that $\hat{u}^0 \in Z_h^\perp$ is given and that we solve for $u^1 \in V_h$ via

$$a(u^1, v_h) = (\nabla \cdot \hat{u}^0, \nabla \cdot v_h)_{L^2(\Omega)} - \sigma a(\hat{u}^0, v_h) \quad \forall v_h \in V_h,$$

which we can do since $a(\cdot, \cdot)$ is coercive on V_h . Then for all $v_h \in Z_h$

$$a(u^1, v_h) = (\nabla \cdot \hat{u}^0, \nabla \cdot v_h)_{L^2(\Omega)} - \sigma a(\hat{u}^0, v_h) = 0$$

since both terms vanish. Thus $u^1 \in Z_h^\perp$. Moving on, we can solve for $u^n \in V_h$ via

$$(2.13) \quad a(u^n, v_h) = (\nabla \cdot \hat{u}^{n-1}, \nabla \cdot v_h)_{L^2(\Omega)} - \sigma a(\hat{u}^{n-1}, v_h) \quad \forall v_h \in V_h.$$

By induction, $a(u^n, v_h) = 0$ for all $v_h \in Z_h$, so that $u^n \in Z_h^\perp$ for all $n > 0$.

To start the process, we can solve for $u^0 \in V_h$ via

$$(2.14) \quad a(u^0, v) = (\nabla \cdot w, \nabla \cdot v)_{L^2(\Omega)} \quad \forall v \in V_h,$$

where we must pick some w where $\nabla \cdot w \neq 0$. In practice, we chose

$$(2.15) \quad w = (\sin(\omega x), \cos(\omega y)),$$

for $\omega \in \mathbb{Z}$, although other initializations worked as well. We then set

$$(2.16) \quad \hat{u}^0 = (\|u^0\|_V)^{-1} u^0.$$

Note that $a(u^0, v) = 0$ for all $v \in Z_h$, which means that $u^0 \in Z_h^\perp$. The division in (2.16) provides a natural check that $u^0 \neq \mathbf{0}$.

2.3. Eigenvalue bounds. The eigenvalues λ_i are bounded above since

$$\|\nabla \cdot v_h\|_{L^2}^2 \leq C a(v_h, v_h) \quad \forall v_h \in V.$$

This is obvious for the gradient form (2.3) with $C \leq d$, where d is the dimension of Ω . For the ε form (2.8), it follows by the Korn inequality [9, §11.2]. A good estimate of C can be obtained computationally since it is the largest eigenvalue of (2.9). In all computational examples here, using the gradient form (2.3), $C = 1$, apparently due to the homogeneous Dirichlet boundary conditions in V . Using the ε form (2.8), which is equivalent to (2.3) by Korn's inequality, would change the computational results here by at most a constant factor. When homogeneous Dirichlet boundary conditions are enforced, it is known [46, (13.12)] that the forms (2.8) and (2.3) produce identical values for divergence-free functions.

Thus we can shift by a constant σ independent of h to ensure that $\lambda_i^\sigma < 0$ for all i . The algorithm (2.12) is the power method for $A^{-1}B - \sigma I$, and it will generically converge to the eigenvector associated with the most negative eigenvalue, provided $\sigma > \frac{1}{2}\lambda_N$, and so it will generically converge to λ_1^σ . Taking $\sigma = 0$ will converge to the largest eigenvalue λ_N , since $0 < \lambda_1$. We found that taking $\sigma = 0.6$ gave acceptable convergence.

2.4. Effect of round-off error. It is essential to start the iteration (2.12) with $\hat{u}^0 \in Z_h^\perp$. To see what goes wrong otherwise, write the algorithm in (2.12) as

$$u^{k+1} = c_k(A^{-1}B - \sigma I)u^k,$$

where $c_k = 1/\|u^k\|_V$. Suppose that $u^0 = v^0 + w^0$ where $v^0 \in Z_h^\perp$ and $w^0 \in Z_h$. Then $u^k = v^k + w^k$ where $v^k \in Z_h^\perp$ and $w^k \in Z_h$, and

$$v^{k+1} = c_k(A^{-1}B - \sigma I)v^k, \quad w^{k+1} = c_k(-\sigma I)w^k.$$

The reason is that $A^{-1}B$ maps Z_h^\perp into itself and Z_h to the zero vector. Define $C_k = \prod_{i=0}^{k-1} c_i$. Then

$$v^k = C_k(A^{-1}B - \sigma I)^k v^0, \quad w^k = C_k(-\sigma I)^k w^0.$$

In seeking the smallest eigenvalue λ_1 , we will need to take σ as large as at least half of the largest eigenvalue λ_N . Thus w^k can become significant even if w^0 is on the order of round-off error. Once w^k becomes dominant, the Rayleigh quotient in (2.12)

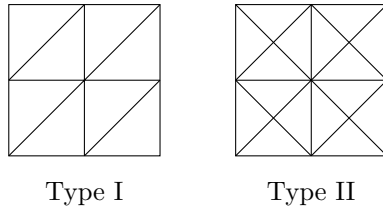


FIG. 2.2. Two types of regular meshes in two dimensions. The Type II mesh is also known as the Malkus split.

defining λ^k will go to zero. Thus it is necessary to monitor the projection z^k of u^k onto Z_h and to project u^k onto Z_h^\perp (by simply subtracting z^k) when the divergence-zero component is too large. This may need to be done for $k = 0$ as well.

The projection $z^k \in Z_h$ satisfies

$$a(z^k, v) = a(u^k, v) \quad \forall v \in Z_h.$$

The projection z^k can be computed via the iterated penalty method. Some care is required in using the iterated penalty method to do this, since it will be slow to converge if the inf-sup constant is small. But this appears to work well in practice, albeit with a large number of iterations required when the inf-sup constant is smaller.

2.5. Full algorithm. We now summarize the full algorithm. First we compute \hat{u}^0 via (2.14) and (2.16), where w is given in (2.15). Next, we solve for u^n via (2.13), $n \geq 1$. Then we project u^n onto Z_h using the iterated penalty method [9, §13.1]. To compute the projection of u^n onto Z_h , we solve for $z^\ell, w^\ell \in V_h$ such that

$$(2.17) \quad \begin{aligned} a(z_\ell, v) + \rho(\nabla \cdot z_\ell, \nabla \cdot v) &= a(u^n, v) - (\nabla \cdot w_\ell, \nabla \cdot v) \quad \forall v \in V_h \\ w_{\ell+1} &= w_\ell + \rho z_\ell, \end{aligned}$$

where we start with $w_0 = 0$. The parameter ρ is the penalty parameter enforcing the incompressibility constraint; in our computations we set $\rho = 10^4$. We terminate the iteration on ℓ when

$$(2.18) \quad \|\nabla \cdot z_\ell\|_{L^2(\Omega)} \leq \tau,$$

where we picked $\tau = 10^{-14}$ in our computations. Then $z_\ell \approx \Pi_{Z_h} u^n$, and if

$$\|\nabla z_\ell\|_{L^2(\Omega)} \geq \zeta \|\nabla u^n\|_{L^2(\Omega)},$$

we update $u^n = u^n - z_\ell$. In our computations, we picked $\zeta = 10^{-12}$. Once u^n has been computed, we define

$$(2.19) \quad \lambda^{n+1} = \frac{(\nabla \cdot u^n, \nabla \cdot u^n)}{a(u^n, u^n)}, \quad \hat{u}^n = (\|u^n\|_V)^{-1} u^n.$$

This iteration is continued while $|\lambda^{n+1} - \lambda^n| > \epsilon$, where ϵ is a pre-specified tolerance, with $\epsilon = 10^{-8}$ in our computations.

2.6. 2D tests. To verify the algorithm, we compare with known results. We summarize some known results in two and three dimensions in Table 2.1. In Table 2.2, we give results for Lagrange elements of degree $k = 1, 2$ in two dimensions on Malkus

TABLE 2.1

Mesh restrictions for V_h constructed with continuous piecewise polynomials of degree k , and $\Pi_h = \nabla \cdot V_h$. Here d is the dimension of Ω . In the lowest-order case $k = 1$ in two dimensions, the velocity approximation is optimal order despite the fact that the inf-sup constant deteriorates.

d	k	inf-sup	mesh restrictions
2	1	no, but	optimal velocity approximation on Malkus splits [33, 40]
2	1	yes	Powell–Sabin splits [13, 20, 53]
2	2	yes	some crossed triangles required [39] or Alfeld splits [22, 17]
2	3	yes	under certain conditions [23]
2	≥ 4	yes	p -robust when no nearly singular vertices [48, 49, 24, 1]
3	≥ 1	yes	Worsey–Farin splits [13]
3	≥ 3	yes	Alfeld splits [52, 22, 17]
3	≥ 6	yes	only one family of meshes known [54]

TABLE 2.2

Computation of inf-sup constants on Malkus splits (Type II meshes) in two dimensions. The shift parameter in (2.11) was set to $\sigma = 0.6$. The mesh size N refers to the $N \times N$ mesh of quadrilaterals before subdivision. The parameter ω determines the initial eigenvector approximation defined in (2.15). Iterations were continued until the change in eigenvalue was less than 10^{-7} .

degree k	N	ω	iterations	inf-sup λ_1	restarts
1	5	5	47	4.08×10^{-1}	0
1	5	10	40	4.08×10^{-1}	0
1	5	100	51	4.08×10^{-1}	1
1	10	10	258	1.13×10^{-2}	1
1	20	10	642	2.98×10^{-3}	1
2	10	10	193	1.49×10^{-1}	13
2	20	10	189	1.48×10^{-1}	14
2	40	10	187	1.48×10^{-1}	19

splits (Type II meshes in the nomenclature of [28] as shown in Figure 2.2), for various mesh sizes. A Malkus split mesh starts with a quadrilateral subdivision and creates a triangulation by subdividing each quadrilateral by adding the two diagonals connecting opposite vertices. On Malkus splits, for $k \geq 2$, the inf-sup constant is bounded and converges relatively rapidly in our tests, but for $k = 1$, the inf-sup constant goes to zero with a rate equal to one over the mesh size parameter [39]. The column “iterations” lists the number of iterations of the power method required to achieve a change in λ less than 10^{-8} . The column “restarts” lists the number of times the projection z_ℓ was subtracted from u^n .

In Table 2.3, we give results for Lagrange elements of degree $k = 2, 3, 4$ in two dimensions on Type I meshes, that is, meshes consisting of 45-degree right triangles (Figure 2.2). The results match the theory indicated in Table 2.1: the inf-sup constant degenerates for $k = 2, 3$, but does not for $k = 4$. There is renewed interest in the low order cases due to the emergence of the grad-div penalized Taylor–Hood method [10, 31, 32]. The approximations from these methods tend to divergence free functions as the penalty is increased, and the low-order Taylor–Hood methods are

TABLE 2.3

Computation of inf-sup constants on Type I meshes (see Figure 2.2) in two dimensions. The shift parameter in (2.11) was set to $\sigma = 0.6$. The mesh size N refers to the $N \times N$ mesh of quadrilaterals before subdivision. The parameter ω determines the initial eigenvector approximation defined in (2.15). Iterations were continued until the change in eigenvalue was less than 10^{-7} for $k = 3$ and $k = 4$, but we had to continue iterations until the change in eigenvalue was less than 10^{-10} for $k = 2$ to obtain a reliable second digit.

degree k	N	ω	iterations	inf-sup λ_1	restarts
2	8	10	13577	1.60×10^{-3}	29
2	16	10	50690	4.08×10^{-4}	129
2	32	10	19851	1.07×10^{-4}	19397
2	64	10	54650	2.75×10^{-5}	54649
3	3	10	790	8.46×10^{-3}	11
3	5	10	768	3.52×10^{-3}	8
3	10	10	1858	9.50×10^{-4}	15
4	5	10	585	2.59×10^{-2}	12
4	10	10	789	2.60×10^{-2}	17
4	20	10	1265	2.60×10^{-2}	28

widely used. It has been known that divergence-free quadratics on Type I meshes have reduced approximation order (this is equivalent to reduced approximation for C^1 piecewise cubic approximation for scalar functions [12]). But so far we know of no estimates for controlled degeneration of the inf-sup constants on general meshes.

2.7. 3D tests. Mesh restrictions in three dimensions for Scott–Vogelius elements are not fully understood. Our computations for Freudenthal meshes are summarized in Table 2.4. They reveal a surprising fact: on this mesh family, the inf-sup constant is bounded for degrees $k \geq 4$, whereas Zhang [54] was able to prove inf-sup stability only for $k \geq 6$. Neilan [36, Proposition 6.5] extends this to more general meshes that satisfy a special condition, which he states as a conjecture, but still for $k \geq 6$. The results in Table 2.4 lead us to make Conjecture 1.

2.8. Size of $\nabla \cdot V_h^k$. In general, $\nabla \cdot V_h^k \subset DG_h^{k-1}$, the latter space being all discontinuous piecewise polynomials of degree $k-1$. In two dimensions, these spaces can be very close in size, differing because of singular vertices and the mean zero constraint due to the homogeneous boundary conditions on V_h^k . But in three dimensions, much less is known. The difference between $\nabla \cdot V_h^k$ and DG_h^{k-1} is known to be quite large for Freudenthal meshes. The constraints on the latter space required to be satisfied to be in the former space are listed in [54, page 691]. For a single cube subdivided by 6 tetrahedra, the dimension of the quotient space is 67 for $k = 6$. We should note that there is a typographical error in equation (3.67) in [54], which should read instead [56]

$$\dim P_h = n^3(k+2)(k+1)k - 3kn(n^2 + n + 2) + 5.$$

Note that $\dim DG_h^{k-1} = n^3(k+2)(k+1)k$, so the number of constraints (the dimension of the quotient space) is $3kn(n^2 + n + 2) - 5$. The algorithm proposed by Rognes [41] can be used to compute the number of constraints on general meshes.

2.9. More general elements. The algorithm described and tested here can be used more generally for computing inf-sup constants. The only restriction is that

TABLE 2.4

Computation of inf-sup constants for various polynomial degrees k in three dimensions on the Freudenthal meshes depicted in Figure 2.1. The shift parameter in (2.11) was set to $\sigma = 0.6$. The mesh size N refers to the $N \times N \times N$ mesh of cubes before subdivision. Iterations were continued until the change in eigenvalue was less than 10^{-7} for $k = 4$ and $k = 5$, but we had to continue iterations until the change in eigenvalue was less than 10^{-8} for $k = 3$.

degree k	N	iterations	inf-sup λ_1	restarts
3	2	1026	5.75×10^{-4}	4
3	3	3400	4.26×10^{-4}	14
3	4	4445	2.93×10^{-4}	29
3	5	6044	2.11×10^{-4}	2048
3	6	7732	1.59×10^{-4}	4863
4	2	802	4.28×10^{-3}	7
4	3	2067	4.13×10^{-3}	16
4	4	1961	4.22×10^{-3}	16
4	5	1325	4.27×10^{-3}	12
4	6	1380	4.26×10^{-3}	12
5	2	1004	6.46×10^{-3}	12
5	3	1003	6.59×10^{-3}	13
5	4	877	6.34×10^{-3}	12
5	5	938	6.26×10^{-3}	13
5	6	978	6.23×10^{-3}	13

$$\Pi_h = \nabla \cdot V_h.$$

3. Space decompositions for the kernel of the divergence. Our second conjecture relates to multigrid solvers for (1.2). In the nearly incompressible regime, the equation becomes nearly singular, and standard multigrid methods break down. A key breakthrough for such problems was made by Schöberl [43], who devised conditions on the relaxation and prolongation operators that guarantee that a multigrid method is parameter-robust in the nearly-singular regime.

3.1. Background. The key condition for the relaxation is best stated in terms of space decompositions and subspace corrections [51]. The multigrid relaxation method we employ will be induced by a space decomposition

$$(3.1) \quad V_h = \sum_{i=1}^J V_i$$

where an equation for an approximation to the error is solved over each subspace V_i and the updates combined additively or multiplicatively. Each V_i is assumed small enough so that direct solvers can be afforded. For example, if $V_h = \text{span}\{\phi_1, \phi_2, \dots, \phi_N\}$, and each V_i is chosen to be $V_i = \text{span}\{\phi_i\}$, then combining the updates additively would yield the Jacobi relaxation, while combining multiplicatively would yield the Gauss–Seidel relaxation. In a domain decomposition approach, each V_i could be taken as the functions supported on one subdomain of a given parallel decomposition of the mesh, combined with a suitable global coarse space. Another important example is to define each V_i as the functions with support on the patch of cells surrounding each vertex,

the so-called *vertex-star* space decomposition: this arises in k -robust preconditioners for symmetric and coercive problems [38, 44], as the Arnold–Falk–Winther (AFW) relaxation for $H(\operatorname{div})$ and $H(\operatorname{curl})$ [3], and in Reynolds-robust preconditioners for the Navier–Stokes equations [6, 16].

Let us consider an abstract nearly singular problem, following Lee et al. [29]. For $\varepsilon > 0$, consider the finite-dimensional linear variational problem: find $u \in V_h$ such that

$$(3.2) \quad a_0(u, v) + \varepsilon^{-1} a_1(u, v) = (f, v) \text{ for all } v \in V_h,$$

where a_0 is symmetric and coercive, and a_1 is symmetric but only positive semi-definite. In the context of (1.2), $a_1(u, v) = (\nabla \cdot u, \nabla \cdot v)_{L^2}$. Define the kernel

$$(3.3) \quad \mathcal{N} = \{u \in V_h : a_1(u, v) = 0 \text{ for all } v \in V_h\}.$$

In our context, these are divergence-free functions in the finite element space. A key condition that must be satisfied by the space decomposition for parameter-robustness in ε is [29, Assumption (A1)]:

$$(3.4) \quad \mathcal{N} = \sum_{i=1}^J (\mathcal{N} \cap V_i).$$

In other words, when challenged with a divergence-free function, it must be possible to decompose this as the sum of functions with the i^{th} summand drawn from the divergence-free functions in V_i ¹. The space decomposition that induces Jacobi or Gauss–Seidel relaxation does not generally satisfy (3.4), because the intersection $\mathcal{N} \cap V_i = \{0\}$ for typical finite element methods where the standard bases used are not divergence-free.

3.2. Space decompositions from de Rham complexes. One way to devise space decompositions that satisfy (3.4) is by inspecting discrete subcomplexes of a suitable underlying Hilbert complex. For concreteness, consider $\Omega \subset \mathbb{R}^2$, with Ω simply connected. The Stokes complex [27] is given by

$$(3.5) \quad \mathbb{R} \xrightarrow{\operatorname{id}} H^2(\Omega) \xrightarrow{\operatorname{curl}} [H^1(\Omega)]^2 \xrightarrow{\operatorname{div}} L^2(\Omega) \xrightarrow{\operatorname{null}} 0.$$

This complex is discretized with a discrete subcomplex

$$(3.6) \quad \mathbb{R} \xrightarrow{\operatorname{id}} \Sigma_h \xrightarrow{\operatorname{curl}} V_h \xrightarrow{\operatorname{div}} Q_h \xrightarrow{\operatorname{null}} 0,$$

where $\Sigma_h \subset H^2(\Omega)$, $V_h \subset [H^1(\Omega)]^2$, and $Q_h \subset L^2(\Omega)$. These complexes have the property that the kernel of an operator curl , div , or null is a subspace of the range of the preceding operator, e.g. that $\ker(\operatorname{div}) \subset \operatorname{range}(\operatorname{curl})$ [2]. The complex is called *exact* if the kernel of an operator is precisely the range of the preceding operator. The Stokes complex is exact if the domain Ω is simply connected, and this property is inherited by (3.6) if constructed appropriately (with bounded cochain projections).

In our context, these complexes are useful because they offer a crisp characterization of $\mathcal{N} = \ker(\operatorname{div})$. Let $\Sigma_h = \operatorname{span}\{\psi_1, \dots, \psi_M\}$ and $V_h = \operatorname{span}\{\phi_1, \dots, \phi_N\}$. If $u_h \in \mathcal{N}$, then $u_h = \operatorname{curl} \Psi_h$ for $\Psi_h \in \Sigma_h$ by exactness of (3.6). Expanding Ψ_h in terms of its basis functions

$$(3.7) \quad \Psi_h = \sum_{i=1}^M c_i \psi_i$$

¹This decomposition must also be stable, but we shall not elaborate here.

yields an expression for u_h

$$(3.8) \quad u_h = \sum_{i=1}^M c_i \operatorname{curl} \psi_i.$$

Suppose the space decomposition (3.1) is chosen as $J = N + M$ with

$$(3.9) \quad V_i = \begin{cases} \operatorname{span}(\operatorname{curl} \psi_i) & i = 1, \dots, M \\ \operatorname{span}(\phi_{i-M}) & i = M + 1, \dots, M + N. \end{cases}$$

This decomposition would satisfy (3.4), with $V_i \cap \mathcal{N} = V_i$ for $i \leq M$ or $V_i \cap \mathcal{N} = \{0\}$ for $i > M$.

Solving the problem (3.2) over $\operatorname{span}\{\operatorname{curl} \psi_i\}$ reduces to solving a problem in a locally-supported subspace of Σ_h , as described in Hiptmair [25] and Hiptmair–Xu [26] for the L^2 de Rham complex. However, for the Stokes complex in three dimensions, explicit constructions of Σ_h are poorly understood. The alternative approach (which we refer to as Pavarino–Arnold–Falk–Winther, PAFW) is to construct the space decomposition using only knowledge of the supports of the basis functions ψ_i . For example, if Σ_h exists with the property that each basis function ψ_i is a polynomial of degree $k + 1$ supported on a certain region of the domain $\operatorname{supp}(\psi_i)$, then we may choose $\{V_j\}$ so that each V_j captures all polynomials of degree k on one $\operatorname{supp}(\psi_i)$. In this way, $\forall i = 1, \dots, M \exists j$ s.t. $\operatorname{curl} \psi_i \in V_j$, and (3.4) will also be satisfied, without needing to explicitly construct Σ_h or $\{\psi_i\}_{i=1}^M$. Only knowledge (or conjecture) of the supports is required.

To illustrate the PAFW construction, consider the case of the Scott–Vogelius element pair with $k \geq 4$ and $d = 2$. This element constructs V_h with $[\operatorname{CG}_k]^d$ and Q_h with DG_{k-1} on a mesh \mathcal{T}_h . The corresponding C^1 -conforming finite element for Σ_h is the Morgan–Scott element of degree $k + 1$ [34], which is not implemented in general purpose finite element software, preventing the application of (3.9). The Morgan–Scott element employs (among others) degrees of freedom at the vertices of the mesh, and the basis function associated with such a degree of freedom will have support over the patch of cells sharing that vertex. This suggests the following vertex-star space decomposition, which we now describe. Let ν_1, \dots, ν_J be the vertices of \mathcal{T}_h . The subspaces are given by

$$(3.10) \quad V_j = \{v_h \in V_h : \operatorname{supp}(v_h) \subset \operatorname{star}(\nu_j)\},$$

where the star operation of a simplex p returns the union of all simplices containing p as a subsimplex [35, §2]. In other words, when applied to a vertex ν_j , the star is the union of the cells and edges (and faces in $d = 3$) containing ν_j , as well as ν_j itself. In [34], it is proven that the Morgan–Scott basis functions are each supported in $\operatorname{star}(\nu_j)$ for some j , provided $k \geq 4$. Thus (3.10) also satisfies the kernel decomposition (3.4). Numerical experiments indicate that (3.10) does indeed yield ε -robust convergence for $k \geq 4$, as expected from the Morgan–Scott theory, while it does not for $k < 4$ [14, §4.2].

There are other examples where the vertex-star space decomposition does not yield ε -robust convergence. For $k = 1$ on Malkus splits, the basis with smallest possible support has support that is larger than $\operatorname{star}(\nu_j)$, although it is in

²This space decomposition relates to that proposed by Hiptmair [25]. As written it is not robust in k , but (experimentally) can be made so by applying suitable block Jacobi methods in V_h and Σ_h .

$\text{star}(\text{closure}(\text{star}(\nu_j)))$ [47], where the star of a set of simplices is the union of their stars, and closure is defined in [14].

3.3. Second conjecture. The preceding discussion indicates that one may experimentally investigate whether Σ_h permits a basis with support captured by the stars of the vertices, by applying the multigrid algorithm and observing whether the convergence is ε -robust or not.

The continuous Stokes complexes in 3D [15] is given by

$$(3.11) \quad \mathbb{R} \xrightarrow{\text{id}} H^2(\Omega) \xrightarrow{\text{grad}} H^1(\text{curl}, \Omega) \xrightarrow{\text{curl}} [H^1(\Omega)]^3 \xrightarrow{\text{div}} L^2(\Omega) \xrightarrow{\text{null}} 0.$$

Here

$$(3.12) \quad H^1(\text{curl}, \Omega) := \{v \in [H^1(\Omega)]^3 : \text{curl } v \in [H^1(\Omega)]^3\}.$$

This complex is discretized with a discrete subcomplex

$$(3.13) \quad \mathbb{R} \xrightarrow{\text{id}} S_h \xrightarrow{\text{grad}} \Sigma_h \xrightarrow{\text{curl}} V_h \xrightarrow{\text{div}} \Pi_h \xrightarrow{\text{null}} 0.$$

The space S_h consists of C^1 piecewise polynomials of degree $k + 2$. The space Σ_h consists of continuous vector-valued piecewise polynomials of degree $k + 1$ which have a continuous curl. Note that $(S_h)^3 \subset \Sigma_h$.

The potential space Σ_h is known on special meshes (Alfeld or Worsey–Farin splits) in three dimensions [17, 21, 8]. We are not aware of any results that characterize Σ_h on Freudenthal meshes.

Based on the numerical experiments we will report, we make the following conjecture:

CONJECTURE 2. *Let $V_h \subset [H^1(\Omega)]^3$ be constructed with continuous Lagrange elements of degree k , and let $\Sigma_h \subset H^1(\text{curl}, \Omega)$ be the space preceding V_h in a subcomplex of the three-dimensional Stokes complex.*

- (a) *For $k = 4$, there does not exist a local basis for Σ_h , supported on the stars of vertices, on the Freudenthal meshes depicted in Figure 2.1.*
- (b) *For $k \geq 5$, there exists a local basis for Σ_h , supported on the stars of vertices, on the Freudenthal meshes depicted in Figure 2.1.*

Our evidence for **Conjecture 2(b)** is not as strong as for **Conjecture 2(a)**. For example, the results of Schöberl [43] are not necessary and sufficient, so robustness could occur for some other reason. But lack of robustness implies lack of a suitable local basis.

3.4. Numerical experiments. We provide numerical evidence for **Conjecture 2**. We solve the problem: find $u \in V_h \subset [H_0^1(\Omega)]^3$ such that:

$$(3.14) \quad (\nabla u, \nabla v)_{L^2(\Omega)} + \gamma(\nabla \cdot u, \nabla \cdot v)_{L^2(\Omega)} = (1, v)_{L^2(\Omega)} \quad \forall v \in V_h.$$

The problem becomes nearly singular as $\gamma \rightarrow \infty$. Here V_h is constructed with continuous Lagrange elements of degree k . We employ the solver denoted in Figure 3.1. The relaxation on each level is one application of damped Richardson iteration preconditioned by the additive Schwarz method with vertex-star subspaces chosen as (3.10). The damping factor is set to $1/M$ where M is the maximum number of patches that a given vertex is contained in. Here $M = 3$ for $d = 2$ and $M = 4$ for $d = 3$. The coarse grid solve was computed with CHOLMOD [11] via PETSc [5]. The code was run in serial.

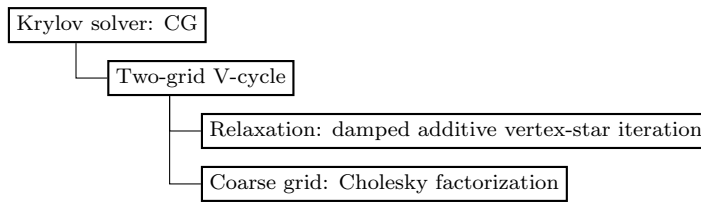


FIG. 3.1. Solver diagram for (3.14).

TABLE 3.1

Iteration counts for (3.14) on a uniform refinement of a Type I 4×4 mesh. The iteration counts are γ -robust for $k \geq 4$, but not for $k < 4$.

$k \setminus \gamma$	10^0	10^1	10^2	10^3	10^4	10^5
2	11	17	35	54	87	100
3	10	13	23	49	62	83
4	9	10	13	13	13	12
5	9	10	11	12	11	10

3.5. Two dimensions. The convergence results for the solver depicted in Figure 3.1 are shown in Table 3.1, as a function of k and γ . The Krylov method was terminated when the unpreconditioned residual was reduced by 8 orders of magnitude. The coarse mesh was a Type I mesh [28] of size 4×4 . The main observation is that $k \geq 4$ is required for γ -robust performance. This matches well with the existing theory described above: the key property that changes between these two cases is the existence of the Morgan–Scott element for Σ_h with a basis supported on vertex-stars for $k \geq 4$.

3.6. Three dimensions. In three dimensions we again choose $V_h = [CG_k]^d$. We employ an analog of a Type I coarse mesh of size $4 \times 4 \times 4$, with one refinement. We show iteration counts for the solution of the problem of (3.14) in Table 3.2. As in two dimensions, the solver was terminated when the unpreconditioned residual was reduced by 8 orders of magnitude. These results lead us to Conjecture 2.

TABLE 3.2

Iteration counts for (3.14) on 2 uniform refinements of a Type I $4 \times 4 \times 4$ mesh. The iteration counts are γ -robust for $k \geq 5$, but not for $k < 5$.

$k \setminus \gamma$	10^0	10^1	10^2	10^3	10^4	10^5
2	14	23	52	118	300	849
3	11	16	29	66	173	458
4	11	13	19	26	54	110
5	11	12	16	19	20	19
6	10	11	14	15	16	15
7	10	11	13	14	14	13

Note that our Conjecture 1 is that the global inf-sup condition holds on this mesh family for $k \geq 4$. Thus there is a gap for $k = 4$: we conjecture that the global inf-sup condition holds, but that there is not a basis for the potential space supported on vertex-stars.

4. Conclusions. Our computational experiments have suggested two conjectures regarding the three-dimensional Stokes complex on Freudenthal meshes. We conjecture that the inf-sup condition holds for a velocity space V_h consisting of continuous piecewise polynomials of degree k and pressure space $\nabla \cdot V_h$ for $k \geq 4$, and that there is a local basis for the associated potential space Σ_h for $k \geq 5$.

5. Acknowledgements. The authors would like to thank Michael Neilan, Charles Parker, Florian Wechsung, Umberto Zerbinati, and Shangyou Zhang for useful discussions.

Appendix A. Freudenthal triangulation of the unit cube.

For concreteness we describe the Freudenthal triangulation of the unit cube $[0, 1]^3$. Define vertices with coordinates

$$\begin{aligned} \mathbf{v}_1 &= (0, 0, 0), & \mathbf{v}_2 &= (1, 0, 0), & \mathbf{v}_3 &= (1, 1, 0), & \mathbf{v}_4 &= (1, 1, 1), \\ \mathbf{v}_5 &= (0, 1, 0), & \mathbf{v}_6 &= (1, 0, 1), & \mathbf{v}_7 &= (0, 1, 1), & \mathbf{v}_8 &= (0, 0, 1). \end{aligned}$$

Then the six cells (tetrahedra) \mathbf{c}_i have vertices

$$\begin{aligned} \mathbf{c}_1 &= [\mathbf{v}_1, \mathbf{v}_2, \mathbf{v}_3, \mathbf{v}_4], & \mathbf{c}_2 &= [\mathbf{v}_1, \mathbf{v}_3, \mathbf{v}_4, \mathbf{v}_5], & \mathbf{c}_3 &= [\mathbf{v}_1, \mathbf{v}_2, \mathbf{v}_4, \mathbf{v}_6], \\ \mathbf{c}_4 &= [\mathbf{v}_1, \mathbf{v}_4, \mathbf{v}_5, \mathbf{v}_7], & \mathbf{c}_5 &= [\mathbf{v}_1, \mathbf{v}_4, \mathbf{v}_6, \mathbf{v}_8], & \mathbf{c}_6 &= [\mathbf{v}_1, \mathbf{v}_4, \mathbf{v}_7, \mathbf{v}_8]. \end{aligned}$$

It is well known [54, Figure 2] that a standard multigrid subdivision of a Freudenthal triangulation of the unit cube $[0, 1]^3$ yields eight subcubes, each subdivided by a Freudenthal triangulation. In particular, the subdivision of the Freudenthal triangulation of the unit cube $[0, 1]^3$ consists of cutting by the three planes $x = 1/2$, $y = 1/2$, and $z = 1/2$. See [54, section 4] for more information regarding multigrid for these meshes.

REFERENCES

- [1] M. AINSWORTH AND C. PARKER, *Unlocking the secrets of locking: finite element analysis in planar linear elasticity*, Computer Methods in Applied Mechanics and Engineering, 395 (2022), p. 115034, <https://doi.org/10.1016/j.cma.2022.115034>.
- [2] D. N. ARNOLD, *Finite element exterior calculus*, Society for Industrial and Applied Mathematics, 2018, <https://doi.org/10.1137/1.9781611975543>.
- [3] D. N. ARNOLD, R. S. FALK, AND R. WINTHER, *Multigrid in $H(\text{div})$ and $H(\text{curl})$* , Numerische Mathematik, 85 (2000), pp. 197–217, <https://doi.org/10.1007/pl00005386>.
- [4] D. N. ARNOLD AND M. E. ROGNES, *Stability of Lagrange elements for the mixed Laplacian*, Calcolo, 46 (2009), pp. 245–260, <https://doi.org/10.1007/s10092-009-0009-6>.
- [5] S. BALAY, S. ABHYANKAR, M. F. ADAMS, S. BENSON, J. BROWN, P. BRUNE, K. BUSCHELMAN, E. CONSTANTINESCU, L. DALCIN, A. DENER, V. EIJKHOUT, W. D. GROPP, V. HAPLA, T. ISAAC, P. JOLIVET, D. KARPEEV, D. KAUSHIK, M. G. KNEPLEY, F. KONG, S. KRUGER, D. A. MAY, L. C. MCINNES, R. T. MILLS, L. MITCHELL, T. MUNSON, J. E. ROMAN, K. RUPP, P. SANAN, J. SARICH, B. F. SMITH, S. ZAMPINI, H. ZHANG, H. ZHANG, AND J. ZHANG, *PETSc/TAO users manual*, Tech. Report ANL-21/39 - Revision 3.17, Argonne National Laboratory, 2022.
- [6] M. BENZI AND M. A. OLSHANSKII, *An augmented Lagrangian-based approach to the Oseen problem*, SIAM Journal on Scientific Computing, 28 (2006), pp. 2095–2113, <https://doi.org/10.1137/050646421>.
- [7] J. BEY, *Simplicial grid refinement: On Freudenthal’s Algorithm and the optimal number of congruence classes*, Numerische Mathematik, 85 (2000), pp. 1–29, <https://doi.org/10.1007/s002110050475>.
- [8] D. BOFFI, S. GONG, J. GUZMÁN, AND M. NEILAN, *Convergence of Lagrange finite element methods for Maxwell eigenvalue problem in 3D*, IMA Journal of Numerical Analysis, (2023), p. drad053, <https://doi.org/10.1093/imanum/drad053>.

- [9] S. C. BRENNER AND L. R. SCOTT, *The Mathematical Theory of Finite Element Methods*, Springer-Verlag, third ed., 2008.
- [10] M. A. CASE, V. J. ERVIN, A. LINKE, AND L. G. REBHOLZ, *A connection between Scott–Vogelius and grad-div stabilized Taylor–Hood FE approximations of the Navier–Stokes equations*, SIAM Journal on Numerical Analysis, 49 (2011), pp. 1461–1481, <https://doi.org/10.1137/100794250>.
- [11] Y. CHEN, T. A. DAVIS, W. W. HAGER, AND S. RAJAMANICKAM, *Algorithm 887: CHOLMOD, supernodal sparse Cholesky factorization and update/downdate*, ACM Transactions on Mathematical Software, 35 (2008), pp. 1–14, <https://doi.org/10.1145/1391989.1391995>.
- [12] C. DE BOOR AND K. HÖLLIG, *Approximation order from bivariate C^1 -cubics: a counterexample*, Proceedings of the American Mathematical Society, 87 (1983), pp. 649–655, <https://doi.org/10.2307/2043352>.
- [13] M. FABIEN, J. GUZMÁN, M. NEILAN, AND A. ZYTOON, *Low-order divergence-free approximations for the Stokes problem on Worsey–Farin and Powell–Sabin splits*, Computer Methods in Applied Mechanics and Engineering, 390 (2022), p. 114444, <https://doi.org/10.1016/j.cma.2021.114444>.
- [14] P. E. FARRELL, M. G. KNEPLEY, L. MITCHELL, AND F. WECHSUNG, *PCPATCH: Software for the topological construction of multigrid relaxation methods.*, ACM Transactions on Mathematical Software, 47 (2021), pp. 1–22, <https://doi.org/10.1145/3445791>.
- [15] P. E. FARRELL, L. MITCHELL, L. R. SCOTT, AND F. WECHSUNG, *A Reynolds-robust preconditioner for the Scott–Vogelius discretization of the stationary incompressible Navier–Stokes equations*, SMAI Journal of Computational Mathematics, 7 (2021), pp. 75–96, <https://doi.org/10.5802/smai-jcm.72>.
- [16] P. E. FARRELL, L. MITCHELL, AND F. WECHSUNG, *An augmented Lagrangian preconditioner for the 3D stationary incompressible Navier–Stokes equations at high Reynolds number*, SIAM Journal on Scientific Computing, 41 (2019), pp. A3073–A3096, <https://doi.org/10.1137/18M1219370>.
- [17] G. FU, J. GUZMÁN, AND M. NEILAN, *Exact smooth piecewise polynomial sequences on Alfeld splits*, Mathematics of Computation, 89 (2020), pp. 1059–1091, <https://doi.org/10.1090/mcom/3520>.
- [18] D. GALLISTL, *Rayleigh–Ritz approximation of the inf-sup constant for the divergence*, Mathematics of Computation, 88 (2019), pp. 73–89, <https://doi.org/10.1090/mcom/3327>.
- [19] G. H. GOLUB AND Q. YE, *An inverse free preconditioned Krylov subspace method for symmetric generalized eigenvalue problems*, SIAM Journal on Scientific Computing, 24 (2002), pp. 312–334, <https://doi.org/10.1137/S1064827500382579>.
- [20] J. GUZMÁN, A. LISCHKE, AND M. NEILAN, *Exact sequences on Powell–Sabin splits*, Calcolo, 57 (2020), pp. 1–25, <https://doi.org/10.1007/s10092-020-00361-x>.
- [21] J. GUZMÁN, A. LISCHKE, AND M. NEILAN, *Exact sequences on Worsey–Farin splits*, Mathematics of Computation, 91 (2022), pp. 2571–2608, <https://doi.org/10.1090/mcom/3746>.
- [22] J. GUZMÁN AND M. NEILAN, *Inf-sup stable finite elements on barycentric refinements producing divergence-free approximations in arbitrary dimensions*, SIAM Journal on Numerical Analysis, 56 (2018), pp. 2826–2844, <https://doi.org/10.1137/17M1153467>.
- [23] J. GUZMÁN AND L. R. SCOTT, *Cubic Lagrange elements satisfying exact incompressibility*, SMAI Journal of Computational Mathematics, 4 (2018), pp. 345–374, <https://doi.org/10.5802/smai-jcm.38>.
- [24] J. GUZMÁN AND L. R. SCOTT, *The Scott–Vogelius finite elements revisited*, Mathematics of Computation, 88 (2019), pp. 515–529, <https://doi.org/10.1090/mcom/3346>.
- [25] R. HIPTMAIR, *Multigrid method for Maxwell’s equations*, SIAM Journal on Numerical Analysis, 36 (1998), pp. 204–225, <https://doi.org/10.1137/s0036142997326203>.
- [26] R. HIPTMAIR AND J. XU, *Nodal auxiliary space preconditioning in $H(\text{curl})$ and $H(\text{div})$ spaces*, SIAM Journal on Numerical Analysis, 45 (2007), pp. 2483–2509, <https://doi.org/10.1137/060660588>.
- [27] V. JOHN, A. LINKE, C. MERDON, M. NEILAN, AND L. G. REBHOLZ, *On the divergence constraint in mixed finite element methods for incompressible flows*, SIAM Review, 59 (2017), pp. 492–544, <https://doi.org/10.1137/15m1047696>.
- [28] M.-J. LAI AND L. L. SCHUMAKER, *Spline functions on triangulations*, no. 110 in Encyclopedia of Mathematics and its Applications, Cambridge University Press, 2007.
- [29] Y.-J. LEE, J. WU, J. XU, AND L. ZIKATANOV, *Robust subspace correction methods for nearly singular systems*, Mathematical Models and Methods in Applied Sciences, 17 (2007), pp. 1937–1963, <https://doi.org/10.1142/s0218202507002522>.
- [30] A. LINKE, *A divergence-free velocity reconstruction for incompressible flows*, Comptes Rendus Mathematique, 350 (2012), pp. 837–840, <https://doi.org/10.1016/j.crma.2012.10.010>.

- [31] A. LINKE, L. G. REBHOLZ, AND N. E. WILSON, *On the convergence rate of grad-div stabilized Taylor–Hood to Scott–Vogelius solutions for incompressible flow problems*, Journal of Mathematical Analysis and Applications, 381 (2011), pp. 612–626, <https://doi.org/10.1016/j.jmaa.2011.03.019>.
- [32] S. E. MALICK, *A connection between grad-div stabilized FE solutions and pointwise divergence-free FE solutions on general meshes*, SIAM Undergraduate Research Online, 9 (2016), pp. 367–383, <https://doi.org/10.1137/16S015176>.
- [33] D. S. MALKUS AND E. T. OLSEN, *Linear crossed triangles for incompressible media*, in Unification of Finite Element Methods, H. Kardestuncer, ed., vol. 94 of North-Holland Mathematics Studies, North-Holland, 1984, pp. 235–248, [https://doi.org/10.1016/S0304-0208\(08\)72627-6](https://doi.org/10.1016/S0304-0208(08)72627-6).
- [34] J. MORGAN AND L. R. SCOTT, *A nodal basis for C^1 piecewise polynomials of degree $n \geq 5$* , Mathematics of Computation, 29 (1975), pp. 736–740, <https://doi.org/10.2307/2005284>.
- [35] J. R. MUNKRES, *Elements of Algebraic Topology*, CRC Press, 1984.
- [36] M. NEILAN, *Discrete and conforming smooth de Rham complexes in three dimensions*, Mathematics of Computation, 84 (2015), pp. 2059–2081, <https://doi.org/10.1090/S0025-5718-2015-02958-5>.
- [37] M. NEILAN, *The Stokes complex: a review of exactly divergence-free finite element pairs for incompressible flows*, in 75 Years of Mathematics of Computation, vol. 754, American Mathematical Soc., 2020, p. 141, <https://doi.org/10.1090/conm/754>.
- [38] L. F. PAVARINO, *Additive Schwarz methods for the p -version finite element method*, Numer. Math., 66 (1993), pp. 493–515, <https://doi.org/10.1007/BF01385709>.
- [39] J. QIN, *On the convergence of some low order mixed finite elements for incompressible fluids*, PhD thesis, Penn State, 1994.
- [40] J. QIN AND S. ZHANG, *Stability and approximability of the \mathcal{P}_1 – \mathcal{P}_0 element for Stokes equations*, International Journal for Numerical Methods in Fluids, 54 (2007), pp. 497–515, <https://doi.org/10.1002/flid.1407>.
- [41] M. E. ROGNES, *Automated testing of saddle point stability conditions*, in Automated Solution of Differential Equations by the Finite Element Method: The FEniCS Book, A. Logg, K. Mardal, and G. Wells, eds., Springer, 2012, pp. 657–671, https://doi.org/10.1007/978-3-642-23099-8_36.
- [42] A. SAMEH AND Z. TONG, *The trace minimization method for the symmetric generalized eigenvalue problem*, Journal of Computational and Applied Mathematics, 123 (2000), pp. 155–175, [https://doi.org/10.1016/S0377-0427\(00\)00391-5](https://doi.org/10.1016/S0377-0427(00)00391-5).
- [43] J. SCHÖBERL, *Multigrid methods for a parameter dependent problem in primal variables*, Numerische Mathematik, 84 (1999), pp. 97–119, <https://doi.org/10.1007/s002110050465>.
- [44] J. SCHÖBERL, J. M. MELENK, C. PECHSTEIN, AND S. ZAGLMAYR, *Additive Schwarz preconditioning for p -version triangular and tetrahedral finite elements*, IMA Journal of Numerical Analysis, 28 (2008), pp. 1–24, <https://doi.org/10.1093/imanum/drl046>.
- [45] L. R. SCOTT, *Numerical Analysis*, Princeton Univ. Press, 2011.
- [46] L. R. SCOTT, *Introduction to Automated Modeling with FEniCS*, Computational Modeling Initiative, 2018.
- [47] L. R. SCOTT, *C^1 piecewise polynomials satisfying boundary conditions*, Research Report UC/CS TR-2019-18, Dept. Comp. Sci., Univ. Chicago, 2019.
- [48] L. R. SCOTT AND M. VOGELIUS, *Conforming finite element methods for incompressible and nearly incompressible continua*, in Large Scale Computations in Fluid Mechanics, B. E. Engquist, et al., eds., vol. 22 (Part 2), Providence: AMS, 1985, pp. 221–244.
- [49] L. R. SCOTT AND M. VOGELIUS, *Norm estimates for a maximal right inverse of the divergence operator in spaces of piecewise polynomials*, M^2AN (formerly R.A.I.R.O. Analyse Numérique), 19 (1985), pp. 111–143, <https://doi.org/10.1051/m2an/1985190101111>.
- [50] G. W. STEWART, *Matrix Algorithms. Volume II: Eigensystems*, SIAM, 2001.
- [51] J. XU, *Iterative methods by space decomposition and subspace correction*, SIAM Review, 34 (1992), pp. 581–613, <https://doi.org/10.1137/1034116>.
- [52] S. ZHANG, *A new family of stable mixed finite elements for the 3D Stokes equations*, Mathematics of Computation, 74 (2005), pp. 543–554, <https://doi.org/10.1090/S0025-5718-04-01711-9>.
- [53] S. ZHANG, *On the P_1 Powell–Sabin divergence-free finite element for the Stokes equations*, Journal of Computational Mathematics, (2008), pp. 456–470, <http://www.jstor.org/stable/43693550>.
- [54] S. ZHANG, *Divergence-free finite elements on tetrahedral grids for $k \geq 6$* , Mathematics of Computation, 80 (2011), pp. 669–695, <https://doi.org/10.1090/S0025-5718-2010-02412-3>.
- [55] S. ZHANG, *Quadratic divergence-free finite elements on Powell–Sabin tetrahedral grids*, Calcolo, 48 (2011), pp. 211–244, <https://doi.org/10.1007/s10092-010-0035-4>.
- [56] S. ZHANG, private communication, 2023.